Mechanisms and Modeling of Bake-Hardening Steels: Part II. Complex Loading Paths

V. BALLARIN, A. PERLADE, X. LEMOINE, O. BOUAZIZ, and S. FOREST

The strain-path dependence of yield strength and mechanical behavior of bake hardening (BH) steels have been investigated. In addition to standard BH tensile tests, samples have been prestrained in plane tension, equibiaxial tension, and shear. After aging at 170 °C for 20 minutes, tensile and shear tests have been carried out to examine the strain-path dependence of the mechanical behavior. A polycrystalline self-consistent model was introduced to model the strain-path dependence of the BH effect. The aging treatment was simulated by an additional hardening term in the model. Simulations were performed for various strain paths, and the influence of aging on yield strength was examined. Results showed that yield strength increase follows a master curve in agreement with experiments and literature. Strain-path dependence of BH was then modeled by a macroscopic hardening term in order to carry out computations with a finite element (FE) method code. Simulations of the dent test were performed and compared with experiments for aged or unaged BH steels.

DOI: 10.1007/s11661-009-9812-6
© The Minerals, Metals & Materials Society and ASM International 2009

I. INTRODUCTION

BAKE-HARDENABLE steels belong to a class of forming steels used in the automotive industry for outer panels. They are particularly interesting because they provide both good formability and high dent resistance. Indeed, they can offer high yield strength after forming and paint baking even though they initially have a low yield strength before forming. This hardening after paint-baking process is due to a strain-aging phenomenon, which is the interaction between solute carbon and dislocations (formation of Cottrell atmospheres[1]). This effect has been particularly investigated in a previous article.[2]

Descriptions of bake hardenability are usually based on uniaxial tensile tests. First, a test piece is loaded to 2 pct strain, which is a typical amount of strain received by outer panels during stamping. Then, the specimen is baked at 170 °C for 20 minutes to simulate the industrial paint-baking process. Finally, the prestrained and baked specimen is uniaxially tested in the same direction as the prestrain. The bake hardening (BH) is defined as the difference between the lower yield stress after baking and the final flow stress after prestraining, as displayed in Figure 1.

V. BALLARIN, Research Engineer, is with the Automotive Applications Research Center, Arcelor-Mittal Montataire, 60761 Montataire, France. A. PERLADE and X. LEMOINE, Research Engineers, and O. BOUAZIZ, are with the Automotive Products Research Center, Arcelor-Mittal Maizières, Voie Romaine, 57283 Maizières-lès-Metz, France. Contact e-mail: xavier.lemoine@arcelormittal.com S. FOREST, CNRS Research Director, is with Mines ParisTech, Centre des Matériaux, UMR CNRS 7633, 91003 Evry Cedex, France.

Manuscript submitted October 29, 2007.
Article published online April 15, 2009

However, sheet forming process and dent tests lead to strain paths that are very different from pure tension. Actually, stamping and dent tests are close to plane strain or equibiaxial stretching. The effect of aging on tensile tests has been widely studied in literature. It particularly causes the return of a sharp yield point and formation of Lüders bands.[2] On the other hand, the influence of the aging treatment when strain path is changed has been far less investigated. Wilson *et al.*[3] carried out torsional tests with prestraining, aging treatment, and reverse or forward restraining. They found that, for Bauschinger tests, the sharp yield point returns very slowly, if at all, and the Bauschinger effect is reduced by the aging treatment. Other particular tensile tests were performed[4,5] with prestrain in uniaxial tension, baking, and then tensile tests but with an angle from 0 to 90 deg between directions of prestrain and restrain. Except for continuous loading, experiments showed a disappearance of the sharp yield point. However, results are contradictory regarding the aging influence on yield strength: Jun *et al.*[4] found an increase of yield strength whatever the angle between directions of loading, whereas Hiwatashi *et al.*[5] noticed an increase or a slight decrease depending on the angle. Yet, these conclusions have to be put into perspective because the considered materials were not exactly the same, nor were the aging treatment and prestrain level. Biaxial stretching tests, which are close to the strain path occurring during stamping and dent tests, followed by aging and tensile tests, have been conducted,[6,7] but the results are not very conclusive.

The aim of the present work is to model the effect of BH on strain-path changes. Various experiments were conducted with different strain paths on BH steels. The amplitude of strain-path changes was characterized by the scalar product of previous and subsequent plastic

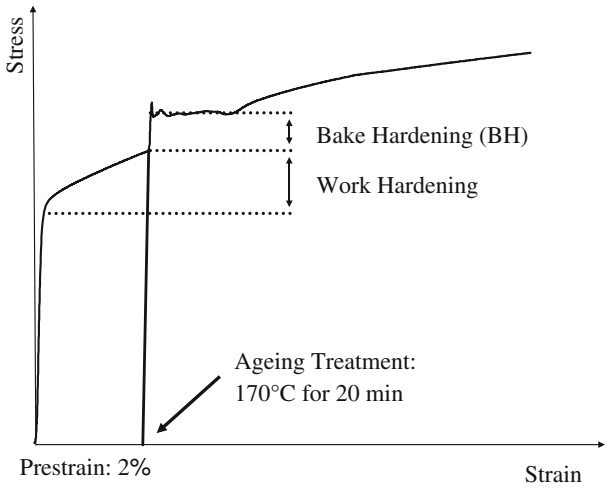

Fig. 1—Schematic diagram of a standard test and definition of BH.

strain tensors. A polycrystalline homogenization model is then introduced in order to get a better understanding of the mechanisms occurring during the restraining of an aged material. The effect of aging treatment on yield strength is investigated and compared with experiments and literature. Then, a macroscopic hardening term reproducing the phenomenon is proposed in order to perform finite element (FE) simulations.

II. MATERIALS AND EXPERIMENTS

Experiments were conducted on two commercially produced BH steels, an aluminum-killed (AlK) one and a Ti-stabilized ultra-low-carbon (ULC) one. The chemical compositions of the steels are detailed in Table I. The average grain diameters were, respectively, 17 and 11 μm for AlK and ULC steels. The thickness of the sheets was 0.7 mm. These steels were designed to give a BH response of the order of 50 MPa for a classic aging treatment (2 pct prestrain, aging at 170 °C for 20 minutes). The typical as-received mechanical properties of the steels are given in Table II.

Prestraining was performed on the AlK steel with uniaxial tension, plane tension, and equibiaxial stretching tests, so that the amount of equivalent prestrain was 2 pct (except for equibiaxial stretching tests where the equivalent prestrain was 4 pct). Plane tension and equibiaxial stretching were conducted using a Marciniak in-plane stretching test.[8] It consists of stamping a testpiece with a hollow punch in order to get a uniformly deformed area at the center. Changing the dimensions of the samples allows attainment of conditions close to plane tension or equibiaxial stretching. Grids were laid on the samples to verify these conditions. For subsequent straining, tensile specimens were cut in the uniformly deformed part of the samples. Second stage tests were carried out in uniaxial tension in the same direction and in a direction at 90 deg to the original tension prestrain. The applied macroscopic strain rate was $2.5{\cdot}10^{-3}$ s^{-1}.

Complementary shear tests were conducted on the ULC steel. Rectangular specimens were fixed by two sets of grips submitted to a parallel displacement.[9] Samples were prestrained at 2 pct in equivalent strain and then restrained in the forward or reverse direction. All the samples were aged at 170 °C for 20 minutes between prestrain and second stage tests.

Table II. Mechanical Properties of the Steels*

Steel	YS (MPa)	UTS (MPa)	UE (Pct)	TE (Pct)
AlK	210	316	19.2	38
ULC	243	316	19.8	33.2

*YS is yield strength, UTS is ultimate tensile strength, UE is uniform elongation, and TE is total elongation.

III. EXPERIMENTAL RESULTS

A scalar parameter useful to characterize strain-path changes has been proposed by Schmitt *et al.*[10] It is defined as

$$\cos\theta = \frac{E_1 : E_2}{(E_1 : E_1)^{1/2}(E_2 : E_2)^{1/2}} \qquad [1]$$

In this formula, E_1 and E_2 represent the prestrain and subsequent plastic strain tensors, respectively. This parameter actually corresponds to the cosine of the angle between E_1 and E_2 in plastic strain space. According to Eq. [1], a monotonous test corresponds to $\cos\theta = 1$ and a Bauschinger test to $\cos\theta = -1$. A deformation sequence is called orthogonal when $\cos\theta = 0$. Examples of tests are given in (Table III).

The effect of strain-path changes on yield stress has been widely investigated in the literature.[10–12] The aim of this work is to concentrate on the effect of the aging treatment on yield stress. For this purpose, responses of the "as-received" and aged materials are considered for a given strain path. The level of the yield stress is studied for a given test characterized by $\cos\theta$.

The first important experimental result is that no Lüders plateau is observed, except of course for uniaxial tensile tests. Even for shear tests, although they correspond to continuous tests, the material response does not present any plateau or yield point elongation. It must be noted that this behavior is valid for the classic aging treatment, that is to say, 170 °C for 20 minutes.

Table I. Chemical Composition (Weight Percent) and Grain Size (μm) of the Steels

Steel	C	Mn	P	Si	S	N	Al	Ti	d (μm)
AlK	0.02	0.196	0.005	0.003	0.015	0.005	0.057	0	17
ULC	0.002	0.713	0.037	0.06	0.009	0.003	0.04	0.013	11

Table III. Tests Commonly Used for the Investigation of the Effect of Aging on Strain-Path Changes; Tests Marked with a Star Were Not Performed in This Investigation; the Angle θ and Its Cosine Are Given for an Isotropic Material; Influence of Anisotropy Can Change Slightly These Values[5]

Test	Denomination	θ	cos θ
Uniaxial tension + uniaxial tension	UT-UT	0 deg	1
Shear in forward direction + shear in forward direction	S +/+	0 deg	1
Plane tension + uniaxial tension in the same direction	PT-UT	30 deg	0.86
Equibiaxial stretching + uniaxial tension	EBS-UT	60 deg	0.5
Uniaxial tension + uniaxial tension in a direction at 45 deg*	UT-UT 45 deg	76 deg	0.25
Plane tension + uniaxial tension in a direction at 90 deg	PT-UT 90 deg	90 deg	0
Uniaxial tension + uniaxial tension in a direction at 90 deg*	UT-UT 90 deg	120 deg	−0.5
Shear in forward direction + shear in reverse direction	S ±	180 deg	−1
Uniaxial tension + uniaxial compression*	UT-UC	180 deg	−1

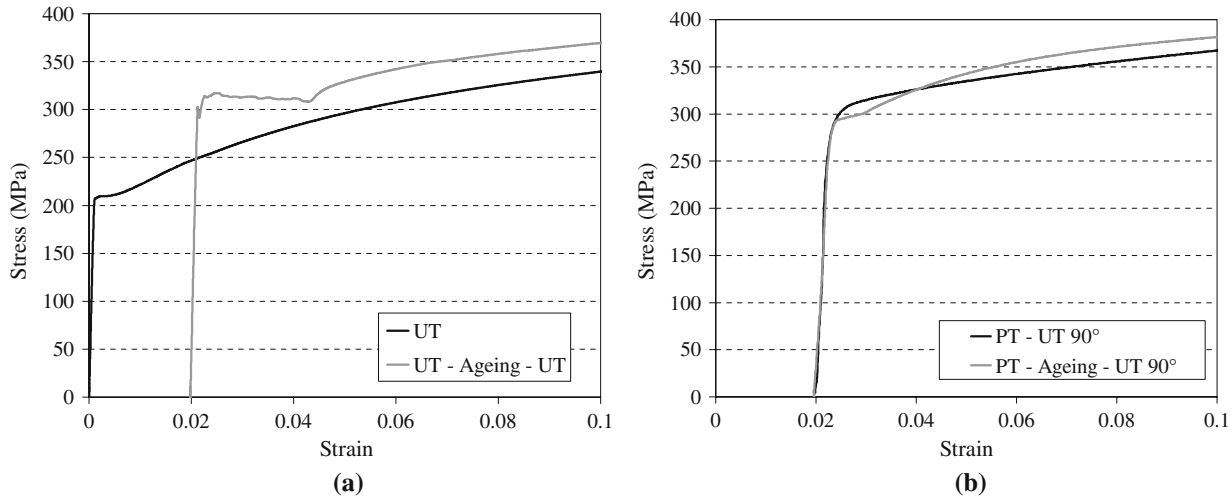

Fig. 2—Influence of aging on the experimental stress-strain responses of the AlK steel: (*a*) UT and (*b*) plane tension followed by uniaxial tensile test at 90 deg of prestrain direction (PT-UT90).

For longer aging, yield point elongation can be observed. This absence of plateau after aging is confirmed by literature for complex strain-path tests.[4–6]

Besides, the effect of aging on yield strength is strongly dependent of the strain path. The yield strength is higher for aged materials than for the as-received one when cos θ is close to 1 or −1. For orthogonal sequences, aging treatment does not increase the yield stress; it can even lead to a slight decrease (Figures 2 and 5). Therefore, a BH treatment, which is supposed to harden the material, can have no influence, or even a negative influence, on yield strength according to strain path.

However, aging increases the flow stress soon after yielding, whatever the strain path. As shown in Figure 2, the aging treatment can have no effect on yield strength, but a hardening phenomenon is noticed in subsequent straining. To investigate this effect, the difference between the stress-strain responses of aged and "as-received" material has been determined for a given cos θ. An exponential law is then calibrated for this difference, which is called "overstress":

$$\Delta\sigma = R_a + Q_a \cdot \left(1 - e^{-b_a \cdot \left(\varepsilon^p - \varepsilon^p_{\text{prestrain}}\right)}\right) \qquad [2]$$

where R_a, Q_a, and b_a are parameters identified for each loading path. This term actually represents the overstress necessary to model the effect of the aging treatment on the response of the material. These overstresses are displayed in Figure 3 for various loading paths. A softening term is introduced to model the Lüders phenomenon in the case of uniaxial tensile tests.[2] For all others tests, the overstress is constant or increasing. A constant overstress means that the aging has an influence on yield strength, but does not modify the flow stress during subsequent straining. For increasing overstresses, the initial value represents the effect of aging on yield strength, and the rest of the curve shows the modification of the flow stress due to aging.

To understand better the strain-path change dependence of BH, the difference between the yield strength of aged and "as-received" steels ΔYS is represented as a function of cos θ in Figure 4. The present tests showed rounded stress-strain curves so that it is difficult to determine the yield strength. A conventional choice is made and the yield stress for a strain of 0.2 pct is used in the present investigation, except for uniaxial tests where the lower yield stress is considered. For cos θ = 1, results of uniaxial tests and shear tests are displayed.

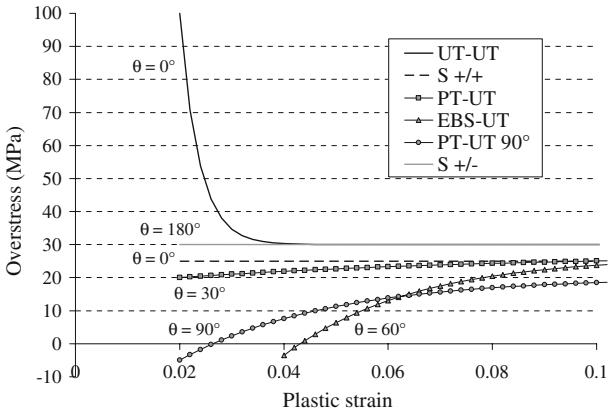

Fig. 3—Overstresses modeling the influence of aging on experimental stress-strain responses for different loading paths.

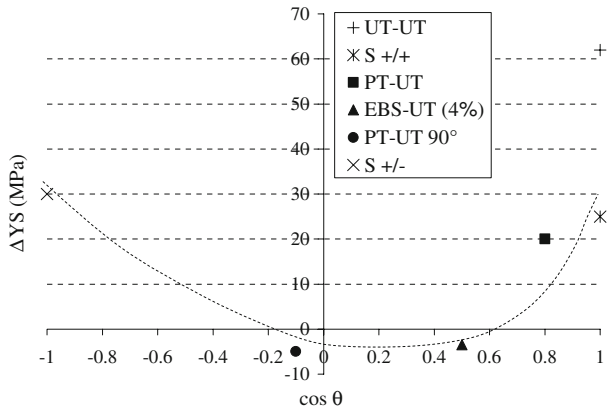

Fig. 4—Influence of aging on experimental yield strengths as a function of cos θ.

The first one actually corresponds to a classic BH test so that ΔYS = BH, as defined in Figure 1.

The following findings can be noted.

(1) When the second strain is in the same direction as prestrain (cos θ = 1), the pinning of dislocations by aging is efficient and increases the yield strength. The Lüders plateau does not appear for shear tests and seems to be strongly structure dependant and related to tensile tests.
(2) When the second strain is in the opposite direction of prestrain (cos θ = −1), the degree of slip reactivation is rather high but the direction is reversed. The pinning of dislocation is quite efficient and yield strength also increases, so that the residual stress developed during prestrain (Bauschinger effect) is partially offset.
(3) When cos θ is close to 0, the aging treatment has almost no influence on the yield strength. The slip systems activated during prestrain are pinned by solute carbon. Yet, slip systems activated during subsequent straining are supposed to be latent during prestrain. Therefore, they are insensitive to carbon pinning, so that the yield strength remains the same. Yet, the aging treatment has pinned some dislocations and has modified the repartition of solute carbon in the matrix, so that the hardening due to forest dislocations is reinforced. As a result, the flow stress is increased soon after yielding.

Experimental results, but also literature,[5] show that ΔYS can be negative for orthogonal sequences. This finding means that the yield strength after aging is lower than the one for the unaged material. This phenomenon could be explained by the presence of internal stresses in the material developed during prestrain. The aging treatment is not hot enough to rearrange the structures of dislocations, but it could lead to the relaxation of these internal stresses, so that ΔYS can be negative.

IV. MODEL

Experimental results show that the BH is strongly dependent on strain-path changes, which can be represented by the parameter cos θ. The activated slip systems during prestrain and subsequent straining will not necessarily be the same. Thus, dislocation pinning can be more or less efficient.

A polycrystalline homogenization model is proposed in order to investigate this phenomenon. Aging phenomena such as Lüders or Portevin Le Chatelier bands have already been observed and studied in single crystals.[13] Thus, modeling the aging of slip systems in order to obtain the macroscopic behavior of aged materials seems to be a reasonable approach. A micromechanical approach has already been used to model the BH effect on steels, but only for tensile tests.[14] The aim of the present work is to study the influence of aging on complex strain paths.

In the following, $\mathbf{Y}$, $\underset{\sim}{Y}$, and $\underset{\approx}{Y}$ correspond to a vector, a second-rank tensor, and a four-rank tensor, respectively.

The aim of the micromechanical approach used is to deduce, through a suitable scale transition, the macroscopic behavior of heterogeneous materials such as metals from the local behavior and the microstructure of the representative volume element (RVE). In the case of metal polycrystals, the RVE is made of grains. The approach of the self-consistent scheme is to consider each grain as an inclusion embedded in an infinite homogeneous matrix submitted to homogeneous boundary conditions.[15] It allows the estimation of the average homogenous stress and the strain fields $\underset{\sim}{\sigma}^g$ and $\underset{\sim}{\varepsilon}^g$ in each grain.

Yet, a self-consistent approach does not take into account the exact shape of grain or the local effect of grain boundaries and of grain size. Precisions on the following model, developed by Berveiller and Zaoui and referred to as the BZ model in this work, can be found in References 15 and 16.

In the case of isotropic elasticity, we have

$$\underset{\sim}{E}^p = \sum_{g\in G} f_g \underset{\sim}{\varepsilon}^{pg} \quad \text{and} \quad \underset{\sim}{\Sigma} = \sum_{g\in G} f_g \underset{\sim}{\sigma}^g = 2\mu\left\{\underset{\approx}{I} + \frac{\nu}{1-2\nu}\underset{\sim}{1}\otimes\underset{\sim}{1}\right\} : \left(\underset{\sim}{E} - \underset{\sim}{E}^p\right) \qquad [3]$$

where μ is the shear modulus and ν is the Poisson ratio. The term $\underset{\sim}{E}^p$ is the macroscopic plastic strain tensor and is equal to the average of the local plastic strain $\underset{\sim}{\varepsilon}^{pg}$ of all grains g. The macroscopic stress $\underset{\sim}{\Sigma}$ can be deduced from Hooke's law. To solve this problem in the case of isotropic elastoplasticity and radial monotonous loading, Berveiller and Zaoui[15] developed a model for a spherical inclusion. The explicit scale transition rule is given by

$$\underset{\sim}{\sigma}^g = \underset{\sim}{\Sigma} + 2\mu(1-\beta)\alpha(\underset{\sim}{E}^g - \underset{\sim}{\varepsilon}^{pg}) \text{ with } \frac{1}{\alpha} = 1 + \frac{3}{2}\mu\frac{\left\|\underset{\sim}{E}^p\right\|}{J_2(\underset{\sim}{\Sigma})} \quad [4]$$

where β is close 0.5, α is the plastic accommodation factor, and $\left\|\underset{\sim}{X}\right\| = \sqrt{\frac{2}{3}\underset{\sim}{X} : \underset{\sim}{X}}$. A detailed description of the meaning of these parameters can be found in Reference 15.

The resolved shear stress on slip system s of grain g is given by

$$\tau^{sg} = \underset{\sim}{\sigma}^g : (\mathbf{m}^{sg} \otimes \mathbf{n}^{sg}) \quad [5]$$

where $\mathbf{m}^{sg}$ and $\mathbf{n}^{sg}$ are, respectively, the slip direction and the normal vector to the slip plane for slip system (s).

The relation between the applied resolved shear stress τ^{sg} and the shear strain rate $\dot{\gamma}^{sg}$ is approximated by[17]

$$\dot{\gamma}^{sg} = \left(\frac{|\tau^{sg}| - r^{sg}}{k}\right)^n \operatorname{sgn}(\tau^{sg}) \quad \text{if } |\tau^{sg}| > \tau_c^{sg}; \quad \dot{\gamma}^{sg} = 0 \text{ otherwise} \quad [6]$$

where r^{sg} is the critical resolved shear stress, and k and n are viscosity parameters. High values of n and low values of K lead to almost rate-independent behavior.

The hardening law is given by

$$r^{sg} = r_0 + Q\sum_u H^{su}\left(1 - e^{-b|\gamma^{ug}|}\right) \quad [7]$$

where r_0, Q, and b are constants and H^{su} is the component of the hardening matrix corresponding to the interaction between the slip system (s) and the slip system (u).

To take into account the aging phenomenon, an additional constitutive law is introduced. The expression of the critical resolved shear stress is modified for the subsequent strain as follows:

$$r^{sg} = r_0 + Q\sum_u H^{su}\left(1 - e^{-b|\gamma^{ug}|}\right) + r_0^{BH} \quad \text{with } r_0^{BH} = BH_{\max}\left(1 - e^{-B\cdot t^{2/3}\cdot(\gamma^{sg})^l}\right) \quad [8]$$

where t is the aging time, and $BH_{\max}$, B, and 1 are parameters.

This equation allows the modeling of the pinning of dislocations implying the need of an overstress to be overcome to activate the aged slip system. This expression, with its dependence with the exponential of $t^{2/3}$, represents the aging kinetics and is comparable with the Harper model.[18] It actually models the kinetics of the first hardening mechanism, as detailed in Reference 2. The dependence on γ^{sg} allows taking into account the aging only for the slip systems activated during prestrain.

For the sake of simplicity, all the coefficients of the hardening matrix were taken to be 1 in the model. Parameters of the hardening law were identified for a uniaxial tension test (Table IV).

The BZ model is suitable for monotonous loading but does not allow the forecasting of mechanical behavior after changes of loading path. Therefore, an extended model, called the β model, has been introduced, which is suitable for complex loading conditions.[16] The β model is used for the prediction of strain-path changes.

The new concentration rule is given by

$$\underset{\sim}{\sigma}^g = \underset{\sim}{\Sigma} + \mu\left(\underset{\sim}{B} - \underset{\sim}{\beta}^g\right) \text{ with } \underset{\sim}{B} = \sum_{g\in G} f_g\,\underset{\sim}{\beta}^g \quad [9]$$

In this formulation, β^g is a local nonlinear kinematic variable bound to grain g, which describes the interaction between grains and the matrix. Its effect is to reduce internal stresses and to give a suitable description of complex loading paths. Its evolution is given by

$$\dot{\underset{\sim}{\beta}}^g = \dot{\underset{\sim}{\varepsilon}}^{pg} - D\cdot J_2\left(\dot{\underset{\sim}{\varepsilon}}^{pg}\right)\cdot\underset{\sim}{\beta}^g \quad [10]$$

where D is a constant.

Simulations were performed with 100 grains with a random orientation. Twenty-four slip systems, sets $\{110\}\langle 111\rangle$ and $\{112\}\langle 111\rangle$, were considered. The parameter D of the β model was identified to obtain the same response as the BZ model for uniaxial tension. Yet, the parameters of this model, particularly the coefficients of the hardening matrix, were not optimized in order to predict the effect of strain-path changes on yield strength. This is confirmed by Figure 5. It displays responses of the β model for four strain paths, without considering the aging. Results are coherent for continuous and Bauschinger tests, but it does not predict the cross effect. Indeed, the yield stress for an orthogonal subsequent strain should be higher than for a monotonous test, whereas the model predicts slightly the contrary.[12] However, Hoc *et al.*[16] showed that such a model is able to predict the mechanical behavior of steel for different loading paths such as plane tension followed by uniaxial tension. Then, various prestraining and subsequent straining were performed, with or without the additional term representing the aging, in order to investigate the influence of cos θ.

Two particular results are presented in Figure 6 for a tensile test (UT-UT) and a plane tension test followed by a uniaxial tension test at 90 deg of prestrain direction

Table IV. Model Parameters

K (MPa·s)	n	r_0 (MPa)	Q (MPa)	b	$BH_{\max}$ (MPa)	B	1	D
10	50	61.8	52.6	5.3	25	20	1.7	448.2

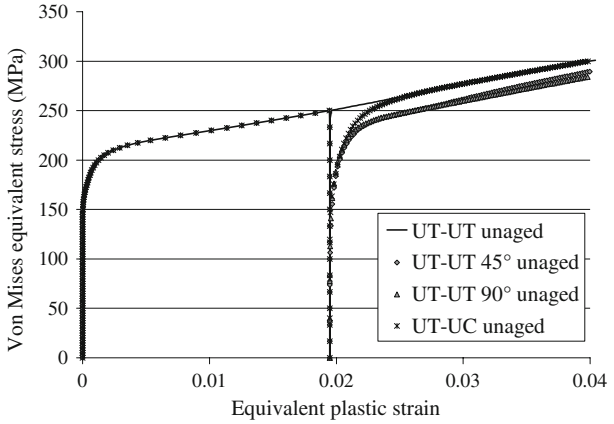

Fig. 5—Simulations with the β model of stress-strain responses for different loading paths without aging.

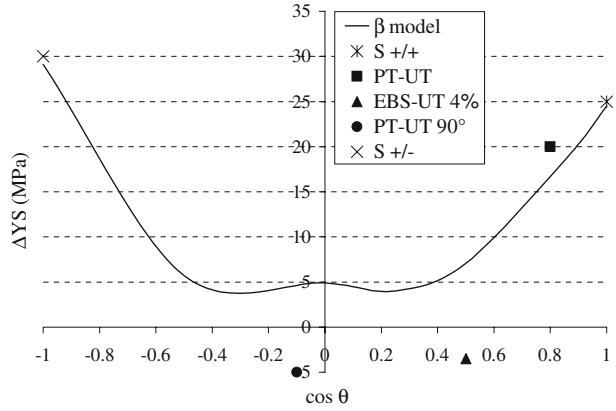

Fig. 7—Modeling of the effect of aging on yield strength.

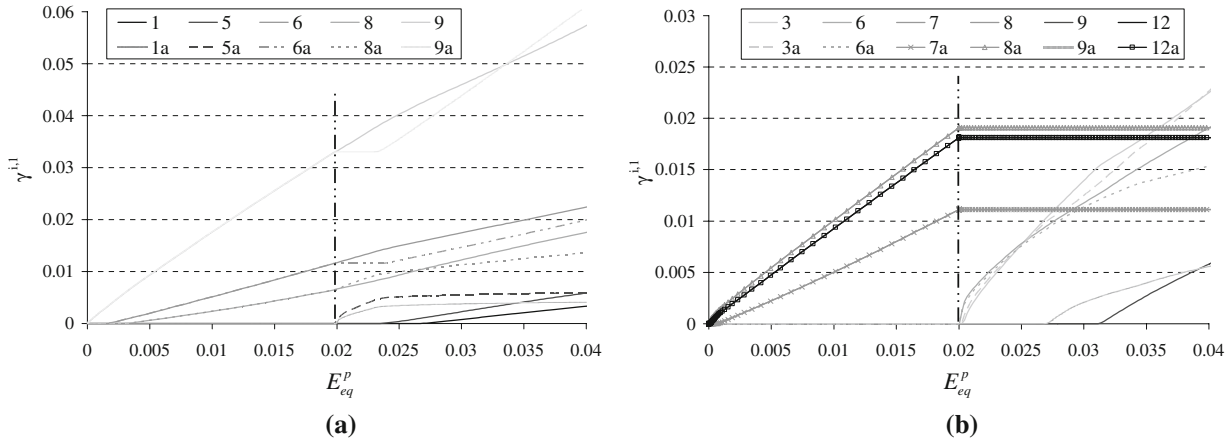

Fig. 6—Activation of slip systems during prestrain and subsequent straining for grain number 1. Slip systems are numbered from $i = 1$ to $i = 12$. Slip systems called "a" correspond to the activation after aging. Unrepresented slip systems were not active during the deformation: (*a*) UT-UT and (*b*) PT-UT90.

(PT-UT 90 deg). This figure displays the activation of slip systems of a given grain ($g = 1$) γ^{sg} as a function of the macroscopic equivalent plastic strain E^p_{eq}. The left-hand part of the curves, until the macroscopic plastic strain equals 2 pct, represents the prestrain. It shows that, in a grain, only a few slip systems are activated among the 12 available. The right-hand part, for E^p_{eq} higher than 2 pct, represents the activation of slip systems during subsequent straining. Figure 6 actually represents the activation of slip systems simulated thanks to the BZ model with 12 slip systems, but results are qualitatively the same as for the β model.

The effect of strain-path changes is particularly enlightened. For a monotonous test (Figure 6(a)), the same systems are active during prestrain and during subsequent straining. Thus, aging has a direct influence on these systems. It can be clearly seen that reactivation of the system number 9 after aging is delayed, because its critical shear stress is higher. The deformation is then accommodated by other slip systems. For an orthogonal test (Figure 6(b)), the activation of slip systems is strongly different. The systems that are activated during prestrain are latent during subsequent straining. Other systems, latent during prestrain, are then activated. Therefore, aging has nearly no influence in this case.

The influence of aging on the yield strength is investigated. To do so, the yield stress for an elastoplastic strain of 0.2 pct is considered. Figure 7 displays the difference between the yield stresses of aged and unaged material ΔYS, as a function of cos θ. Simulations of the influence of aging on strain-path changes are compared with experimental data. A good agreement with experiments and literature[4–6] can be noticed. Particularly, the micromechanical approach reproduces well the important effect of aging during continuous and Bauschinger tests, but also the smaller influence on orthogonal sequences. It has to be noticed that the model, in the present form, cannot take into account the influence of aging on internal stresses, so that the yield strength after aging cannot be lower than the one without aging.

V. IMPLEMENTATION

The previous polycrystal model cannot be used directly in FE simulations because of the large

computing time. The aim of this part is to propose a phenomenological model describing the strain-path dependence of BH, in order to carry out FE simulations. Investigations on the deformation of steels under complex strain paths revealed a complex anisotropic behavior. Teodosiu and Hu[19,20] have used an internal-variable approach based on the understanding of the physical mechanisms of plasticity to develop a model of initial and induced anisotropy of the material. This model was implemented and validated by Haddadi *et al.* for an IF steel under strain-path changes.[21]

The model describing the effect of aging is based on the same idea, that is to say taking into account the anisotropy developed during strain-path changes. Plastic behavior is supposed to be rate independent and the yield condition can be expressed as

$$\Phi\left(\underset{\sim}{\Sigma}\right) = \bar{\Sigma} - Y_0 - R - S \qquad [11]$$

where Y_0 is the initial yield stress and R is the isotropic hardening. The term S represents the contribution of the aging treatment (details are provided subsequently). The equivalent effective stress $\bar{\Sigma}$ is given by the general quadratic function

$$\bar{\Sigma} = \sqrt{\underset{\sim}{s} : \underset{\approx}{M} : \underset{\sim}{s}} \text{ with } \underset{\sim}{s} = \underset{\sim}{\Sigma}' - \underset{\sim}{X} \qquad [12]$$

where σ' is the deviator of the Cauchy stress, X is the kinematics hardening, and $\underset{\approx}{M}$ is a fourth-order tensor representing the texture anisotropy. For BH steels, $\underset{\approx}{M}$ is generally taken to identity (von Mises yield criterion) or in the form of Hill's quadratic yield function.[22] Materials are considered to be isotropic in the present work, so that $\underset{\approx}{M} = \underset{\approx}{1}$.

Associated plasticity is considered:

$$\underset{\sim}{D^p} = \dot{\lambda}\,\underset{\sim}{V}\,;\ \underset{\sim}{V} = \partial\Phi/\partial\underset{\sim}{\Sigma} \qquad [13]$$

where D^p is the plastic strain rate, V is the gradient of the yield function, and $\dot{\lambda}$ is the plastic multiplier.

Hardening is governed by the rate equation having the general form

$$\dot{R} = \rho\dot{\lambda} \quad \text{and} \quad \underset{\sim}{\dot{X}} = \xi\dot{\lambda} \qquad [14]$$

with the initial conditions $R(0) = 0$ and $\underset{\sim}{X}(0) = \underset{\sim}{0}$. The term S follows the same equation: $\dot{S} = \rho_{BH}\dot{\lambda}$.

The hypo-elastic law is given by

$$\underset{\sim}{\dot{\Sigma}} = \underset{\approx}{C} : \left(\underset{\sim}{D} - \underset{\sim}{D^p}\right)$$

where $\underset{\approx}{C}$ is the fourth-order tensor of elastic constants and $\underset{\sim}{D}$ is the total strain rate.

The plastic multiplier is computed using the consistency multiplier and can be written as

$$\dot{\lambda} = \frac{\underset{\sim}{V} : \underset{\approx}{C} : \underset{\sim}{D}}{\underset{\sim}{V} : \underset{\approx}{C} : \underset{\sim}{V} + \underset{\sim}{V} : \xi + \rho + \rho_{BH}}$$

More details on these equations of the elastoplastic behavior can be found in Reference 23.

The term S represents an additional term introduced to model the effect of aging. It is assumed to be equal to 0 during prestrain, and it only plays a role during subsequent straining after aging. This term is aimed at describing the behavior of an aged material, as displayed in Figure 3, according to the amplitude of the strain-path change cos θ. For a given strain path, the overstress is modeled thanks to an exponential law, as described in Eq. [2]. To simplify the model, it is assumed that, after a transitional period after the yield point, the behavior of the aged material is the same whatever the strain path. This means that whatever cos θ, the asymptote of the overstress is the same (Figure 3). Moreover, it is assumed that the length of this transitional step, typically 5 pct strain, is the same whatever the strain path. This assumption allows the determination of the initial slope of the overstress. In a previous article,[2] it has been shown that the effects of grain size and strain rate can be introduced in the coefficient determining the initial slope. Yet, these effects were not investigated in regard to the effect of aging on strain-path changes.

With these assumptions, only the evolution of the yield stress as a function of cos θ has to be studied, because Q_a and b_a can be deduced from R_a (Eq. [2]).

The evolution of S is described by the following equation:

$$S = \Delta R_m + \Delta R_m \cdot \left(1 - \cos^4\theta\right) \cdot e^{-b^* \cdot \left(E^p_{eq} - E^p_{eq_{\text{prestrain}}}\right)} \qquad [15]$$

where ΔR_m and b^* are constants. The term ΔR_m actually represents the asymptote of S, that is to say $R_a + Q_a$. The value of b^* is given by

$$b^* = \frac{1}{x}\ln\left(100\left(1 - \cos^4\theta\right)\right) \qquad [16]$$

The last equation means that b^* is determined so that S has reached its asymptote at 99 pct after x pct strain. The main features of the evolution of S, displayed in Figure 8, are

$$\begin{aligned} S\left(E^p_{eq} = E^p_{eq_{\text{prestrain}}}\right) &= \Delta R_m \cdot \cos^4\theta \quad \text{and} \\ S\left(E^p_{eq} = E^p_{eq_{\text{prestrain}}}\right) &= \Delta R_m \end{aligned} \qquad [17]$$

The initial value of S, for $E^p_{eq} = E^p_{eq_{\text{prestrain}}}$, actually represents the modification of the yield stress due to aging. It allows reproducing the shape of the curve obtained by experiments and polycrystal modeling. For a given initial value depending on cos θ, the material hardens following an exponential law until the asymptote, equal to ΔR_m, is reached. It has to be noticed that this model allows reproduction of the effect of aging observed on shear tests and on strain-path changes but does not take into account the particular Lüders behavior obtained during tensile tests.

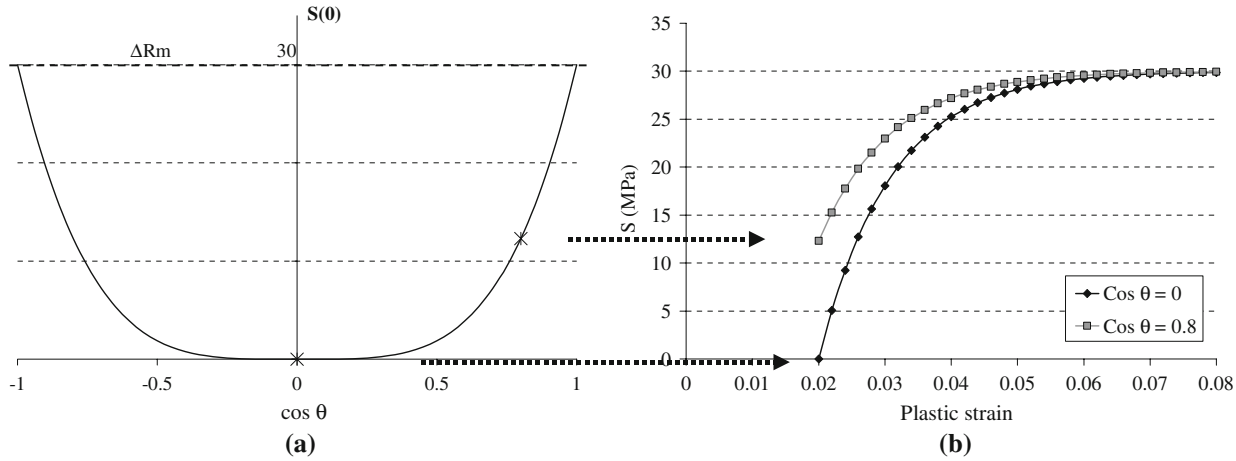

Fig. 8—Main features of the phenomenological hardening term *S*. (*a*) Initial value of *S* as a function of cos θ. (*b*) Evolution of *S* for two values of cos θ as a function of plastic strain.

This model was implemented in the FE code Abaqus v6.4[24] and validated with the shear tests carried out on the ULC steel. The von Mises criterion, Voce isotropic hardening, and no kinematics hardening were used. Simulations of dent resistance are in progress.

VI. CONCLUSIONS

The effect of aging on strain-path changes has been investigated. The study was based on experiments carried out on two BH steels. Various prestrainings and subsequent strains have been performed. Results showed that, for a standard aging treatment of 170 deg for 20 minutes, the sharp yield point and the Lüders plateau returns only during uniaxial tensile tests. For other tests, the yield strength increase due to the aging treatment strongly depends on the amplitude of the strain-path change: it will be important for continuous or Bauschinger tests, whereas it will be close to zero for orthogonal sequences.

A polycrystalline self-consistent approach was used to confirm the experimental results. It particularly enlightened the modification of the activation of slip systems after aging. Simulations performed showed that the yield strength increase follows a master curve in agreement with the experiments and literature.

Eventually, a macroscopic hardening term modeling the phenomenon was proposed in order to carry out FE simulations. Its evolution reproduces the tendency obtained by experiments and polycrystal modeling.

ACKNOWLEDGMENTS

The authors are grateful to M. Soler for carrying out the materials preparation and to J.L. Uriarte and J.H. Schmitt for helpful discussions.

REFERENCES

1. A.H. Cottrell and B.A. Bilby: *Proc. Phys. Soc.*, 1949, vol. 62, pp. 49–62.
2. V. Ballarin, M. Soler, A. Perlade, X. Lemoine, and S. Forest: *Metall. Mater. Trans. A*, 2007, vol. 38A, DOI 10.1007/s11661-009-9813-5.
3. D.V. Wilson and G.R. Ogram: *J. Iron Steel Inst.*, 1968, vol. 206, pp. 911–20.
4. G. Jun and W.F. Hosford: *Metall. Trans. A*, 1986, vol. 17A, pp. 1573–75.
5. S. Hiwatashi and S. Yonemura: *Mater. Sci. Forum*, 2005, vols. 495–497, pp. 1485–92.
6. A. Vicary, W.T. Roberts, and D.V. Wilson: *Z. Metallkd.*, 1993, vol. 84, pp. 702–07.
7. F.D. Bailey, R.P. Foley, and D.K. Matlock: *High-Strength Sheet Steels for Automotive Industry*, Publ. Iron and Steel Society/AIME, Baltimore, MD, 1994, pp. 119–33.
8. Z. Marciniak and K. Kuczynski: *Int. J. Mech. Sci.*, 1967, vol. 9, pp. 609–20.
9. P. Flores, E. Rondia, and A.M. Habraken: *Int. J. Form. Process.*, 2005, vol. 8, pp. 117–37.
10. J.H. Schmitt, E.L. Shen, and J.L. Raphanel: *Int. J. Plast.*, 1994, vol. 10, pp. 535–51.
11. J.H. Schmitt: Ph.D. Thesis, Institut National Polytechnique de Grenoble, Saint-Martin d'Hères, France, 1986 (in French).
12. E.F. Rauch and S. Thuillier: *Mater. Sci. Eng. A*, 1993, vol. A164, pp. 255–59.
13. H. Neuhäuser and A. Hampel: *Scripta Metall. Mater.*, 1993, vol. 29, pp. 1151–57.
14. S. Berbenni, V. Favier, X. Lemoine, and M. Berveiller: *Scripta Mater.*, 2004, vol. 51, pp. 303–08.
15. M. Berveiller and A. Zaoui: *J. Mech. Phys. Solids.*, 1979, vol. 26, pp. 325–44.
16. T. Hoc and S. Forest: *Int. J. Plast.*, 2001, vol. 17, pp. 65–85.
17. G. Cailletaud: *Int. J. Plast.*, 1991, vol. 8, pp. 55–74.
18. S. Harper: *Phys. Rev.*, 1951, vol. 83, pp. 709–12.
19. C. Teodosiu, and Z. Hu: *Proc. Numiforms 95*, Rotterdam, 1995, pp. 173–82.
20. C. Teodosiu and Z. Hu: *Proc. 19th Riso Int. Symp. on Materials Science*, Roskilde, Denmark, 1998, pp. 149–68.
21. H. Haddadi, S. Bouvier, and P. Levée: *J. Phys.*, 2001, vol. 11, pp. 329–37.
22. R. Hill: *Proc. Roy. Soc.*, 1948, vol. A193, pp. 189–297.
23. G. Racz, X. Lemoine, B. Haddag, and F. Abed-Meraim: *Proc 8th Int. Esaform Conf.*, The Romanian Academy Publishing House Bucharest, Cluj-Napoca, Romania, 2005, pp. 293–96.
24. Abaqus, 2004, www.abaqus.com.